Materials Letters 173 (2016) 55–59

Contents lists available at ScienceDirect

Materials Letters

journal homepage: www.elsevier.com/locate/matlet

Synthesis route to δ-FeOOH nanodiscs

Tanja Jurkin [a], Goran Štefanić [b], Goran Dražić [c], Marijan Gotić [b,*]

[a] Ruđer Bošković Institute, Division of Materials Chemistry, Laboratory for Radiation Chemistry and Dosimetry, Bijenička 54, Zagreb, Croatia
[b] Ruđer Bošković Institute, Division of Materials Physics, Laboratory for the Synthesis of New Materials, Bijenička 54, Zagreb, Croatia
[c] National Institute of Chemistry, Hajdrihova 19, SI-1001 Ljubljana, Slovenia

ARTICLE INFO

Article history:
Received 10 December 2015
Received in revised form
13 February 2016
Accepted 4 March 2016
Available online 5 March 2016

Keywords:
Delta-FeOOH
Feroxyhyte
Nanoparticles
Dextran
Gamma-irradiation
Mössbauer

ABSTRACT

δ-FeOOH is a synthetic analogue of a relatively uncommon mineral feroxyhyte (δ′-FeOOH). The conventional syntheses of δ-FeOOH start from the Fe(II) salt and proceed by a rapid oxidation of iron(II) hydroxide with H_2O_2. The new synthesis route to δ-FeOOH nanodiscs reported in this work is based on the γ-irradiation of a deoxygenated iron(III) chloride alkaline aqueous colloidal solution in the presence of 2-propanol and diethylaminoethyl-dextran hydrochloride (DEAE-dextran). γ-irradiation of the colloidal solution enabled the strong reducing conditions thus favouring the reduction of Fe(III) to Fe(II). Under such strong reducing conditions the white suspension characteristic of $Fe(OH)_2$ was formed. When the white suspension came into contact with oxygen from air it rapidly oxidized into stable green-gray suspension characteristic of Fe(II)-Fe(III) hydrochloride known as Green Rust I. In the conventional process of sample isolation the green-gray stable suspension transformed to δ-FeOOH reddish powder that consists of rather uniform regular nanodiscs. The synthesized δ-FeOOH nanodiscs are magnetic and contain a magnetically ordered component in the Mössbauer spectrum at room temperature. It is expected that the results of this work will have a strong impact on finding new synthetic routes to the δ-FeOOH.

1. Introduction

δ-FeOOH is a synthetic analogue of a relatively uncommon mineral feroxyhyte (*δ*′-FeOOH). δ-FeOOH possesses specific structural and magnetic properties and unlike all the other iron oxyhydroxide polymorphs it is magnetic at room temperature [1,2]. However, the magnetic properties of feroxyhyte depend critically on the crystallite and/or particle size [2]. Pollard and Pankhurst [3] have reported that the feroxyhyte (feroxyhite) behaviour is consistent with ferrimagnetism.

δ-FeOOH has been used in various applications [4–8]. For instance, Pereira et al. [5] have reported on the first use of nanostructured δ-FeOOH, with the band gap energy in the visible region, as a promising photocatalyst for the production of hydrogen from water. Pinto et al. [6] have used δ-FeOOH as a heterogeneous catalyst in order to stimulate the degradation of organic contaminates such as a cationic (methylene blue) and an anionic dye (indigo carmine). It has been shown that δ-FeOOH could activate H_2O_2 to produce reactive radicals, which than further promoted the degradation of the dyes. Chagas et al. [7] reported that *δ*-FeOOH released a controlled amount of heat if placed under AC magnetic field, which *δ*-FeOOH classified as promising material for biomedical applications.

A typical synthesis of δ-FeOOH powder involves the precipitation of $Fe(OH)_2$ followed by rapid oxidation with H_2O_2 in an aqueous alkaline suspension. Gotić et al. [9] have reported that strong alkalinity of the mother liquor was an important factor for δ-FeOOH formation via the $Fe(OH)_2$ precursor. Besides, it has been found that a small amount of Fe^{3+}ions present in the $Fe(OH)_2$ precursor before the rapid oxidation of Fe^{2+}ions with H_2O_2 was not critical for the formation of *δ*-FeOOH as a single phase.

In this work, iron(III) precursor was γ-irradiated in the presence of DEAE-dextran, a robust amino-dextran polymer specially designed for biomedical applications and what is more important; it can fully stabilize (disperse) the nanoparticles in an early stage of formation thus forming colloidal solutions rather than suspensions. Quite surprisingly the γ-irradiation of the deoxygenated alkaline aqueous colloidal solution of iron(III) chloride in the presence of DEAE-dextran produced δ-FeOOH nanodiscs as an end product.

2. Materials and methods

2.1. Chemicals

All chemicals were of analytical purity and used as received. Milli-Q deionized water was used. Iron(III) chloride hexahydrate

* Correspondence to: Ruđer Bošković Institute, Division of Materials Physics, Laboratory for the Synthesis of New Materials, Bijenička 54, 10000 Zagreb, Croatia.
E-mail address: gotic@irb.hr (M. Gotić).

http://dx.doi.org/10.1016/j.matlet.2016.03.009
0167-577X/

($FeCl_3 \cdot 6H_2O$), sodium hydroxide (NaOH) and 2-propanol ($(CH_3)_2CHOH$)) were supplied by Kemika, Zagreb. Diethylaminoethyl (DEAE)-dextran hydrochloride (average molecular weight 500.000) was produced by *Sigma*.

2.2. Synthesis and characterization of δ-FeOOH Nanoparticles

0.0934 g (0.35 mmol) of $FeCl_3 \cdot 6H_2O$ and 0.3665 g of DEAE-dextran hydrochloride were dissolved in 20 mL of Milli-Q deionized water and then 0.308 mL of 2-propanol was added. The pH of thus prepared solution was adjusted to 9 by adding 2 M NaOH aqueous solution. The solutions were bubbled with nitrogen in order to remove the dissolved oxygen and then γ-irradiated (without stirring) in a closed glass vial using ^{60}Co source at the Ruđer Bošković Institute. The temperature upon γ-radiation did not exceed 25 °C (room temperature synthesis). The dose rate of γ-radiation was ~7 kGy h^{-1}. The absorbed doses were 113 kGy (sample S1) and 429 kGy (sample S2). The samples were magnetic and they were isolated by decantation with the help of the magnet or by centrifugation followed by washing with ethanol. The isolated samples were dried under vacuum at room temperature and then characterized. The samples were characterized using Electron Microscopies, X-ray powder diffraction and Mössbauer spectroscopy (Section 1 in Supplementary data).

3. Results and discussion

Fig. 1 shows FE SEM images of powder samples S1 and S2 (additional SEM images are shown in Suppl. data). Sample S1 (Fig. 1a) consists of rather uniform thin disc-like (2D morphology) nanoparticles (NPs) having a diameter of about 250 nm (Fig. S0 in Suppl. data). Although the NPs are softly agglomerated, the discrete disc-like NPs are well-visible. The coarse surfaces of NPs suggest the hydrated surfaces of these disc-like NPs. Sample S2 (Fig. 1b) consists of highly stacked disc-like nanoparticles. Due to the high agglomeration some particles have pseudospherical shape. Taking together, the sample S2 consists of pseudospherical nanoparticles that are substructured from laterally aggregated disc-like nanoparticles.

Fig. 2 shows the TEM images and selected area electron diffraction (SAED) patterns of sample S1. Fig. 2a shows the disc-like NPs (nanodiscs) at low magnification. Some of the nanodiscs lie perpendicular to the view. Fig. 2b shows nanodiscs at higher magnification. Fig. 2c shows the high-resolution TEM image of the nanodisc's surface, whereas Fig. 2d shows the corresponding SAED patterns. The nanodisc surface (Fig. 2c) is heterogeneous and consists of small grains. One grain having a diameter of 4 nm is shown. SAED patterns reveal the presence of poorly crystalline α-FeOOH and δ-FeOOH (Fig. 2d and Section S3 in Suppl. data).

The XRD patterns of sample S1 and S2 (Fig. 3, panel A) revealed the presence of δ-FeOOH (feroxyhite, ICDD card No. 77-0247) as a dominant phase and α-FeOOH (goethite, ICDD card 29-0713) as a minor phase. Volume fractions of δ-FeOOH in the samples S1 and S2 were estimated from the results of quantitative crystal phase analysis (Section S3 in Suppl. data) at 0.71(2) and 0.73(2), respectively. Precise lattice parameters determination of δ-FeOOH in samples S1 and S2 (Section S3 in Suppl. data) indicates small increase of the δ-FeOOH lattice parameters in the sample S2. However, both values were close to the values given in the ICDD card 77-0247. The results of line broadening analysis (Section S3 in Suppl. data) indicate the significant size anisotropy in the sample S1 (D_{100} ~ 31 nm and D_{101} ~ 12 nm), which is in line with its anisotropic disc-like morphology (Fig. 1a). In case of the sample S2, the volume averaged domain sizes calculated from the 100 and 101 lines of δ-FeOOH are very similar (D_{100} ~ 16 nm and D_{101} ~ 15 nm), which indicates the dominance of the 3D morphology in this sample. Diffraction lines of α-FeOOH appeared to be very broad, which indicate presence of ultrasmall nanoparticles estimated at ~4.2 nm and ~5.1 nm in samples S1 and S2, respectively (Section S3 in Suppl. data).

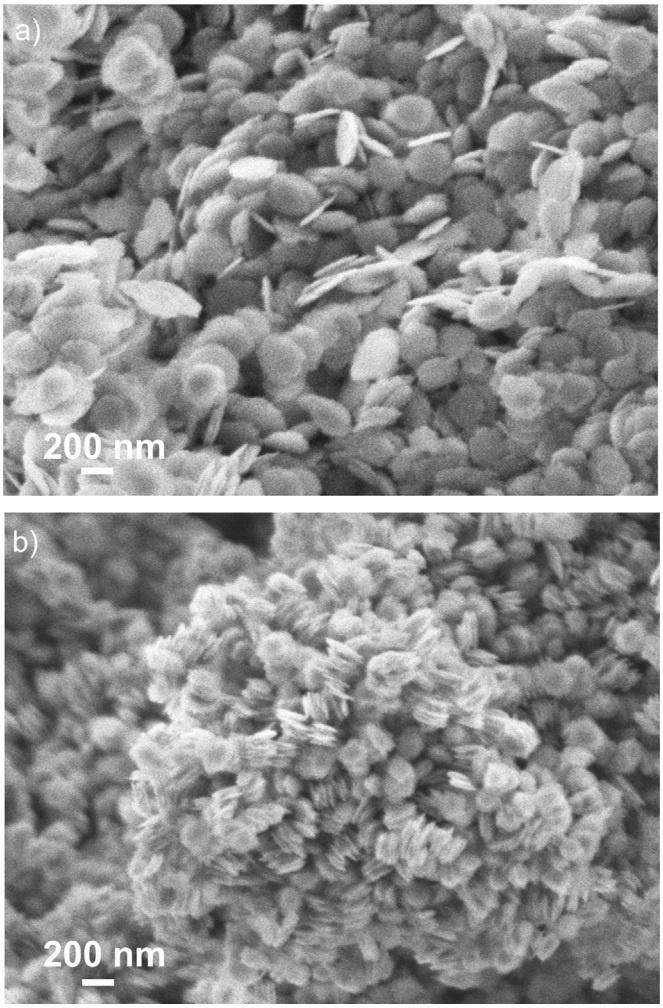

Fig. 1. SEM images of samples S1 (a) and S2 (b) that were γ-irradiated with dose of 113 and 429 kGy, respectively.

The room-temperature Mössbauer spectra of samples S1 and S2 (Fig. 3, panel B) are characterized with a collapsing sextet and a doublet. The collapsing sextet in Mössbauer spectrum can be assigned to FeOOH nanoparticles, whereas the doublet can be assigned to any paramagnetic/superparamagnetic particles [10–12] including α-FeOOH and/or δ-FeOOH. Since the XRD and TEM results confirmed that the sample S1 consisted of the well-crystallized δ-FeOOH having ~29% of poorly crystallized 4–5 nm-α-FeOOH (superparamagnetic range), the collapsing sextets in the Mössbauer spectra can arise from well-crystallized δ-FeOOH. The collapsing nature of sextets may be explained by stacking faults.

Fig. 4 shows the comparison of the conventional (a) and novel synthesis route to δ-FeOOH presented in this work (b). The conventional syntheses of δ-FeOOH start from iron (II) salt and continue by precipitation of $Fe(OH)_2$ under inert atmosphere, which then rapidly oxidizes with H_2O_2 in an aqueous alkaline suspension. The new synthesis route to δ-FeOOH presented in this work started by dissolving iron(III)-chloride salt in DEAE-dextran hydrochloride aqueous solution at pH = 9, the addition of 2-propanol and purging with nitrogen, which favoured the reducing conditions upon γ-irradiation [13–15]. Quite surprisingly the γ-

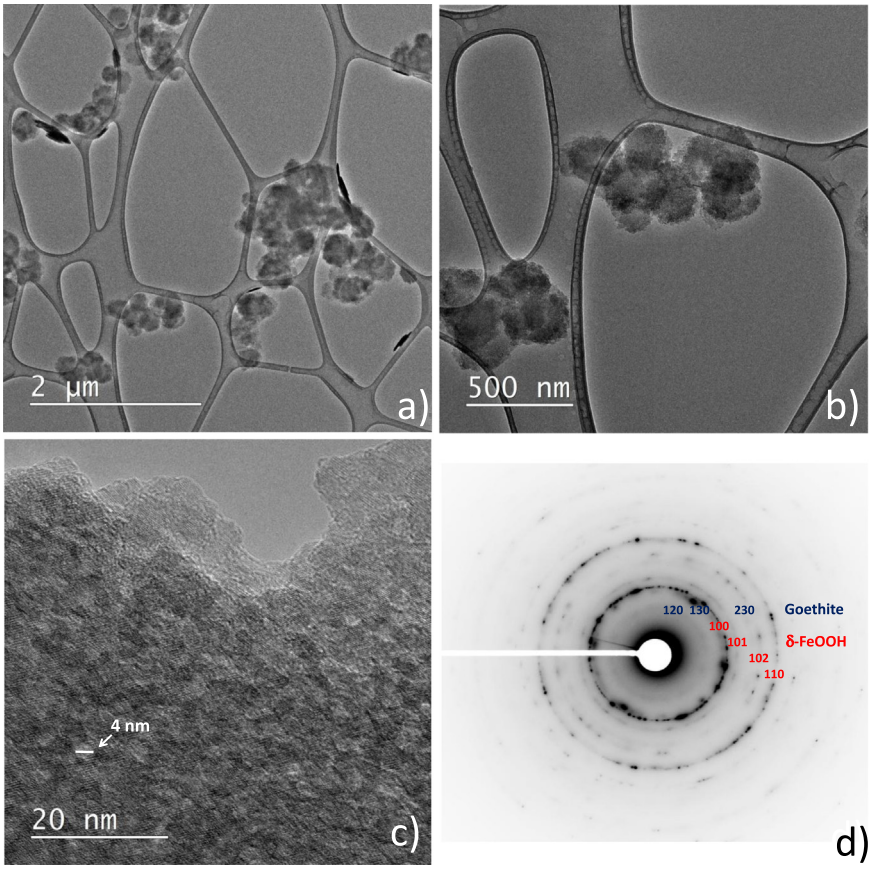

Fig. 2. TEM images (a, b), HRTEM image (c) and corresponding SAED patterns (d) of sample S1.

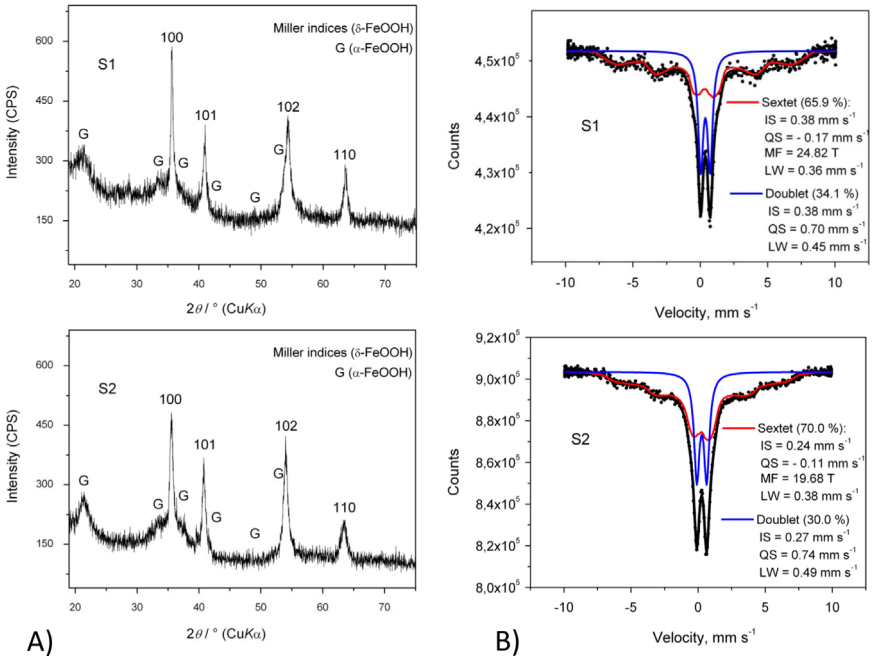

Fig. 3. XRD powder patterns (panel A) and Mössbauer spectra (panel B) of samples S1 and S2 recorded at 20 °C. Mössbauer parameters are given; IS=isomer shift given relative to α-Fe at 20 °C; QS=quadrupole splitting (doublets) or quadrupole shift (sextets); MF=hyperfine magnetic field; LW=line width.

irradiation of the suspension with the dose rate of ~7 kGy and at absorbed dose of 113 kGy produced δ-FeOOH nanodiscs as an end product. At absorbed dose of 31 kGy the pure magnetite was formed. In the absence of γ-irradiation the poorly crystallized α-FeOOH was obtained, whereas the γ-irradiation of the suspension without the DEAE-dextran produced the mixture of α-FeOOH and magnetite (Fe_3O_4). Recently, very small amount of δ-FeOOH has been obtained using γ-irradiation under experimental conditions similar to those in this work, but with different polymers, namely PVP and CTAB [12].

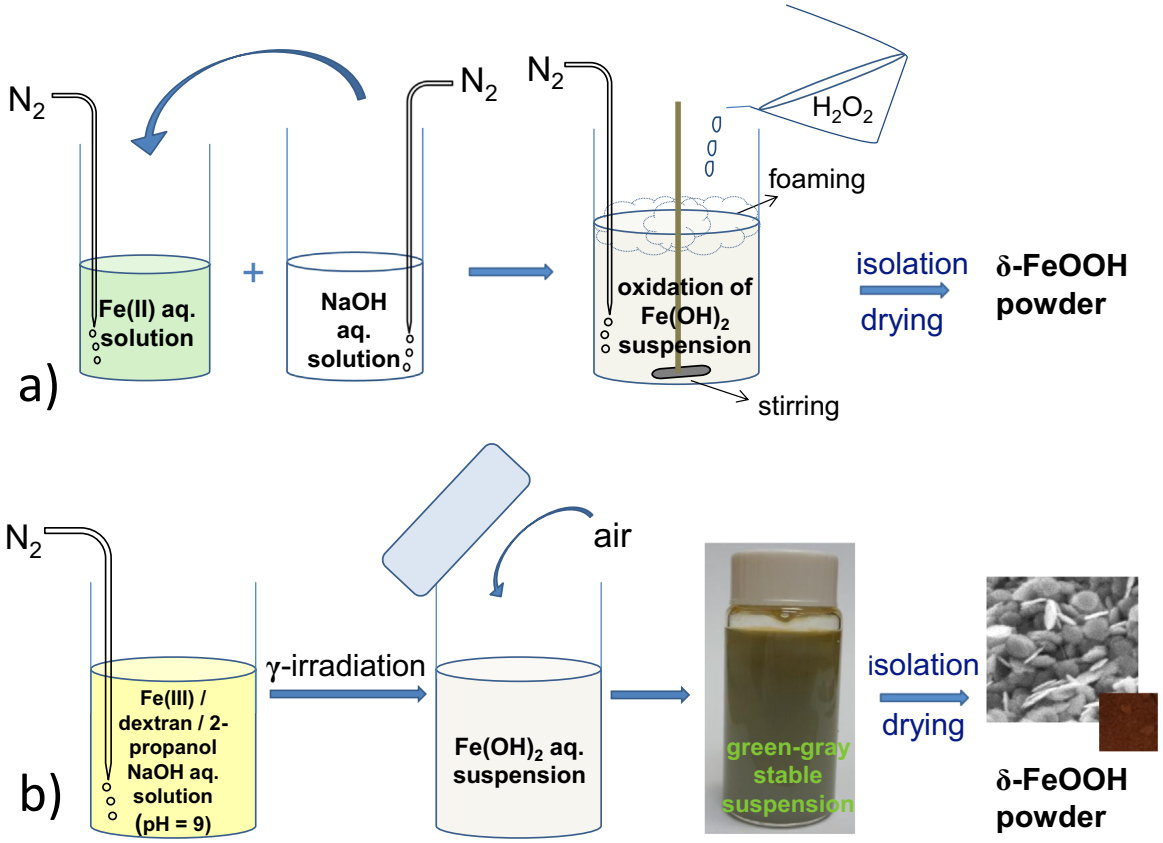

Fig. 4. The comparison of conventional (a) and new synthesis routes to δ-FeOOH powder presented in this work (b).

δ-FeOOH contains iron exclusively as Fe(III) and it is more oxidizing product in comparison to magnetite (Fe_3O_4) that contains 33.3% of iron as Fe(II) [16]. One can conclude that in spite of addition of 2-propanol and deoxygenating of aqueous suspensions there was no reduction of Fe(III) upon γ-irradiation, because the starting precursor and final product exclusively consisted of Fe(III). However, quite contrary in such highly reducing and alkaline conditions the white suspension characteristic of $Fe(OH)_2$ was formed, which after opening the vial cap – thus coming in contact with air – immediately (in a few seconds) turned to a green-gray stable suspension (Fig. 4). The green-gray colour is characteristic of Fe(II)-Fe(III) hydrochloride known as Green Rust I. This chloride-containing Green Rust, GR(Cl^-) is usually prepared by aerial oxidation of $Fe(OH)_2$ suspension in the presence of a slight excess of dissolved ferrous chloride [17]. The formation of GR(Cl^-) involves an *in situ* incorporation of the Cl^- ions from the solution into the interlayers of $Fe(OH)_2$-like hydroxide sheets and a corresponding topotatic oxidation of Fe(II) to Fe(III) without any structural changes [17]. This mechanism explains very well the instantaneous change of colloid colour from white to green-gray after coming in contact with air. In this work the DEAE-dextran hydrochloride is used, which is a robust cationic polymer (positively charged at pH = 9) with Cl^- counter ions. Therefore, the excess of chloride ions needed for GR(Cl^-) formation can be provided by DEAE-dextran. The presence of DEAE-dextran and Cl^- ions in the interlayers of GR(Cl^-) prevented the full oxidation of Fe(II) to Fe(III). Moreover, the iron (oxy)hydroxide NPs are highly stabilized in the colloidal suspension and virtually embedded in the DEAE-dextran polymer matrix (Fig. S5). However, in the conventional process of sample isolation (centrifugation, washing, drying) the DEAE-dextran and Cl^- ions incorporated between the Fe(II)/Fe(III) hydroxide sheets have been almost completely washed out and the green-gray suspension transformed (oxidized) to the δ-FeOOH reddish powder [18,19] that consists of rather uniform regular nanodiscs (Fig. 1).

4. Conclusions

γ-irradiation of alkaline iron(III)-chloride deoxygenated aqueous colloidal solution in the presence of 2-propanol and DEAE-dextran hydrochloride produced stable green-gray suspension, which after isolation transformed to δ-FeOOH reddish powder that consists of rather uniform regular nanodiscs.

γ-irradiation enabled the reduction of Fe(III) to Fe(II), whereas the DEAE-dextran hydrochloride favoured the formation of δ-FeOOH [12]. The synthesized nanoparticles are magnetic and contain a magnetically ordered component in the Mössbauer spectrum at room temperature.

It is expected that the results of this work will have a strong impact on finding new synthetic routes to the δ-FeOOH and its potential use in biomedical applications.

Acknowledgments

This work has been fully supported by Croatian Center of Excellence for Advanced Materials and Sensing Devices. Financial support from the Slovenian Research Agency, the research program P2-0393 (Goran Dražić) is acknowledged. We also thank Mr. Jasmin Forić for the help in experimental work and Mr. Igor Sajko for the technical assistance on γ-irradiation.

Appendix A. Supporting information

Supplementary data associated with this article can be found in

the online version at http://dx.doi.org/10.1016/j.matlet.2016.03.009.

References

[1] L. Carlson, U. Schwertmann, Natural occurrence of Feroxyhite (δ-FeOOH), Clays Clay Miner. 28 (1980) 272–280.

[2] M.B. Madsen, S. Mørup, C.J.W. Koch, O.K. Borggaard, A study of microcrystals of synthestic feroxyhite (δ'-FeOOH), Surf. Sci. 156 (1985) 328–334.

[3] R.J. Pollard, Q.A. Pankhurst, Ferrimagnetism in fine Feroxyhite particles, J. Magn. Magn. Mater. 99 (1991) L39–L44.

[4] T.S. Rocha, E.S. Nascimento, A.C. Silva, H.S. Oliveira, E.M. Garcia, L.C.A. Oliveira, et al., Enhanced photocatalytic hydrogen generation from water by Ni(OH)2 loaded on Ni-doped δ-FeOOH nanoparticles obtained by one-step synthesis, RSC Adv. 3 (2013) 20308–20314, http://dx.doi.org/10.1039/C3RA43561J.

[5] M.C. Pereira, E.M. Garcia, A.C. da Silva, E. Lorençon, J.D. Ardisson, E. Murad, et al., Nanostructured δ-FeOOH: a novel photocatalyst for water splitting, J. Mater. Chem. 21 (2011) 10280–10282, http://dx.doi.org/10.1039/C1JM11736J.

[6] I.S.X. Pinto, P.H.V.V. Pacheco, J.V. Coelho, E. Lorençon, J.D. Ardisson, J.D. Fabris, et al., Nanostructured δ-FeOOH: an efficient fenton-like catalyst for the oxidation of organics in water, Appl. Catal. B: Environ. 119–120 (2012) 175–182, http://dx.doi.org/10.1016/j.apcatb.2012.02.026.

[7] P. Chagas, A.C. da Silva, E.C. Passamani, J.D. Ardisson, L.C.A. de Oliveira, J. D. Fabris, et al., δ-FeOOH: a superparamagnetic material for controlled heat release under AC magnetic field, J. Nanopart. Res. (2013), http://dx.doi.org/10.1007/s11051-013-1544-2.

[8] P. Chen, K. Xu, X. Li, Y. Guo, D. Zhou, J. Zhao, et al., Ultrathin nanosheets of feroxyhyte: a new two-dimensional material with robust ferromagnetic behavior, Chem. Sci. 5 (2014) 2251, http://dx.doi.org/10.1039/c3sc53303d.

[9] M. Gotić, S. Popović, S. Musić, Formation and characterization of δ-FeOOH, Mater. Lett. 21 (1994) 289–295.

[10] M. Gotić, S. Musić, Mössbauer, FT-IR and FE SEM investigation of iron oxides precipitated from $FeSO_4$ solutions, J. Mol. Struct. 834–836 (2007) 445–453, http://dx.doi.org/10.1016/j.molstruc.2006.10.059.

[11] M. Gotić, S. Musić, Synthesis of Nanocrystalline iron oxide particles in the iron (III) acetate/alcohol/acetic acid system, Eur. J. Inorg. Chem. (2008) 966–973, http://dx.doi.org/10.1002/ejic.200700986.

[12] T. Jurkin, M. Gotić, G. Štefanić, I. Pucić, Gamma-irradiation synthesis of iron oxide nanoparticles in the presence of PEO, PVP or CTAB, Radiat. Phys. Chem (2016), http://dx.doi.org/10.1016/j.radphyschem.2015.11.019, in press.

[13] M. Gotić, T. Jurkin, S. Musić, From iron(III) precursor to magnetite and vice versa, Mater. Res. Bull. 44 (2009) 2014–2021, http://dx.doi.org/10.1016/j.materresbull.2009.06.002.

[14] T. Jurkin, K. Zadro, M. Gotić, S. Musić, Investigation of solid phase upon γ-irradiation of ferrihydrite-ethanol suspension, Radiat. Phys. Chem. 80 (2011) 792–798, http://dx.doi.org/10.1016/j.radphyschem.2011.02.031.

[15] N. Hanžić, T. Jurkin, A. Maksimović, M. Gotić, The synthesis of gold nanoparticles by a citrate-radiolytical method, Radiat. Phys. Chem. 106 (2015) 77–82, http://dx.doi.org/10.1016/j.radphyschem.2014.07.006.

[16] M. Gotić, G. Košćec, S. Musić, Study of the reduction and Reoxidation of Substoichiometric magnetite, J. Mol. Struct. 924– 926 (2009) 347–354, http://dx.doi.org/10.1016/j.molstruc.2008.10.048.

[17] P.H. Refait, M. Abdelmoula, J.-M.R. Génin, Mechanisms of formation and structure of green rust one in aqueous corrosion of iron in the presence of chloride ions, Corros. Sci. 40 (1998) 1547–1560.

[18] A.A. Olowe, Y. Marie, P. Refait, J.-M. Génin, Mechanism of formation of delta FeOOH in a basic aqueous medium, Hyperfine Interact. 93 (1994) 1783–1788.

[19] K. Hanna, T. Kone, C. Ruby, Fenton-like oxidation and mineralization of phenol using synthetic Fe(II)-Fe(III) green rusts, Environ. Sci. Pollut. Res. 17 (2010) 124–134, http://dx.doi.org/10.1007/s11356-009-0148-y.

Supplementary data

Table of Contents

Section S1 *Instrumental techniques using for characterization of samples*

The morphology of samples were evaluated using a probe Cs corrected Scanning Transmission Electron Microscope (STEM), model ARM 200 CF, and the field emission scanning electron microscope (FE SEM, model JSM-7000F) manufactured by *JEOL Ltd.*. FE SEM was linked to the EDS/INCA 350 (energy dispersive X-ray analyzer) manufactured by *Oxford Instruments Ltd.*

X-ray powder diffraction (XRD) patterns were recorded at 20 ^{o}C using the APD 2000 X-ray powder diffractometer (Cu *K*α radiation) manufactured by ItalStructures.

^{57}Fe Mössbauer spectra were recorded at 20 ^{o}C in the transmission mode. The spectrometer was calibrated at 20 °C using the standard α-Fe foil spectrum. The velocity scale and all the data refer to the metallic α-Fe absorber at 20 °C.

γ-irradiation was performed using a ^{60}Co source located at the Ruđer Bošković Institute, Zagreb, Croatia

Supplementary data

Section 2 Nanodisc size distributions

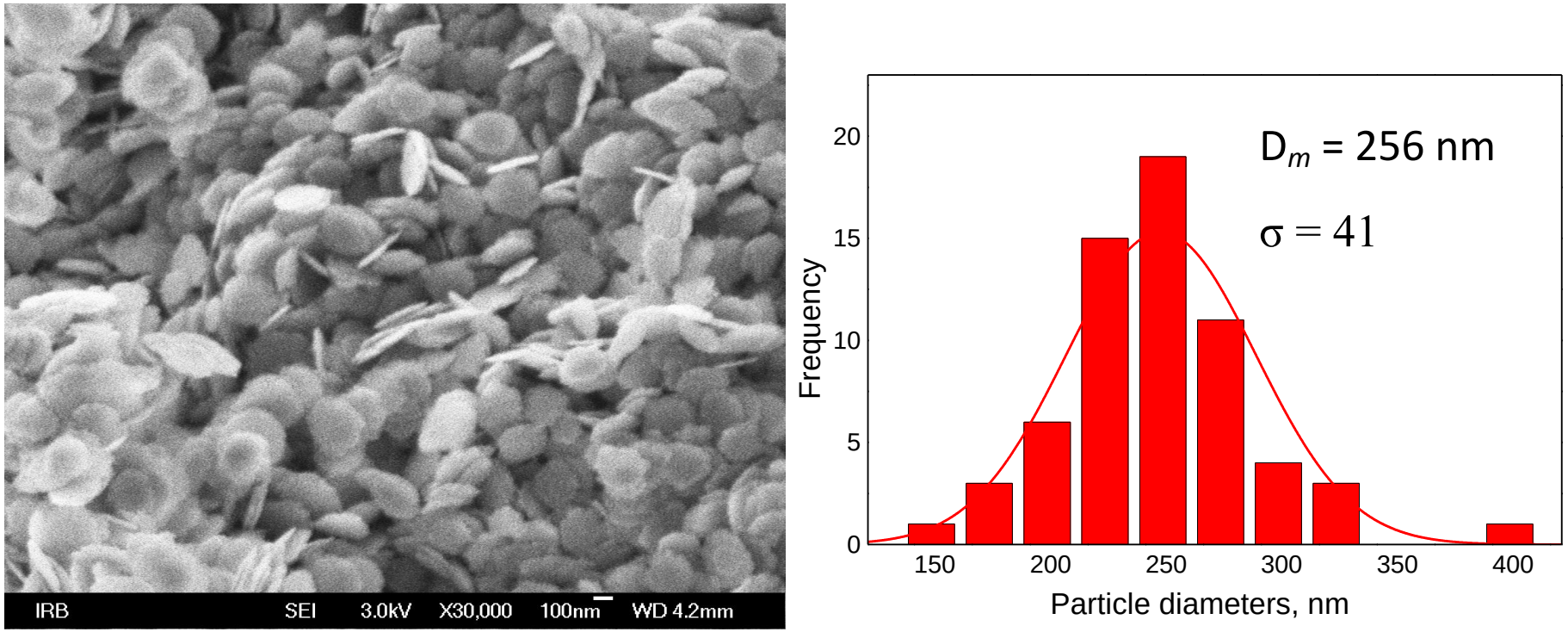

Fig. S0 The mean particle diameter was calculated from the corresponding SEM image using the normal function, where D_m and σ stand for the mean particle diameter and standard deviation, respectively.

Section S2 *SEM and EDS characterizations of samples*

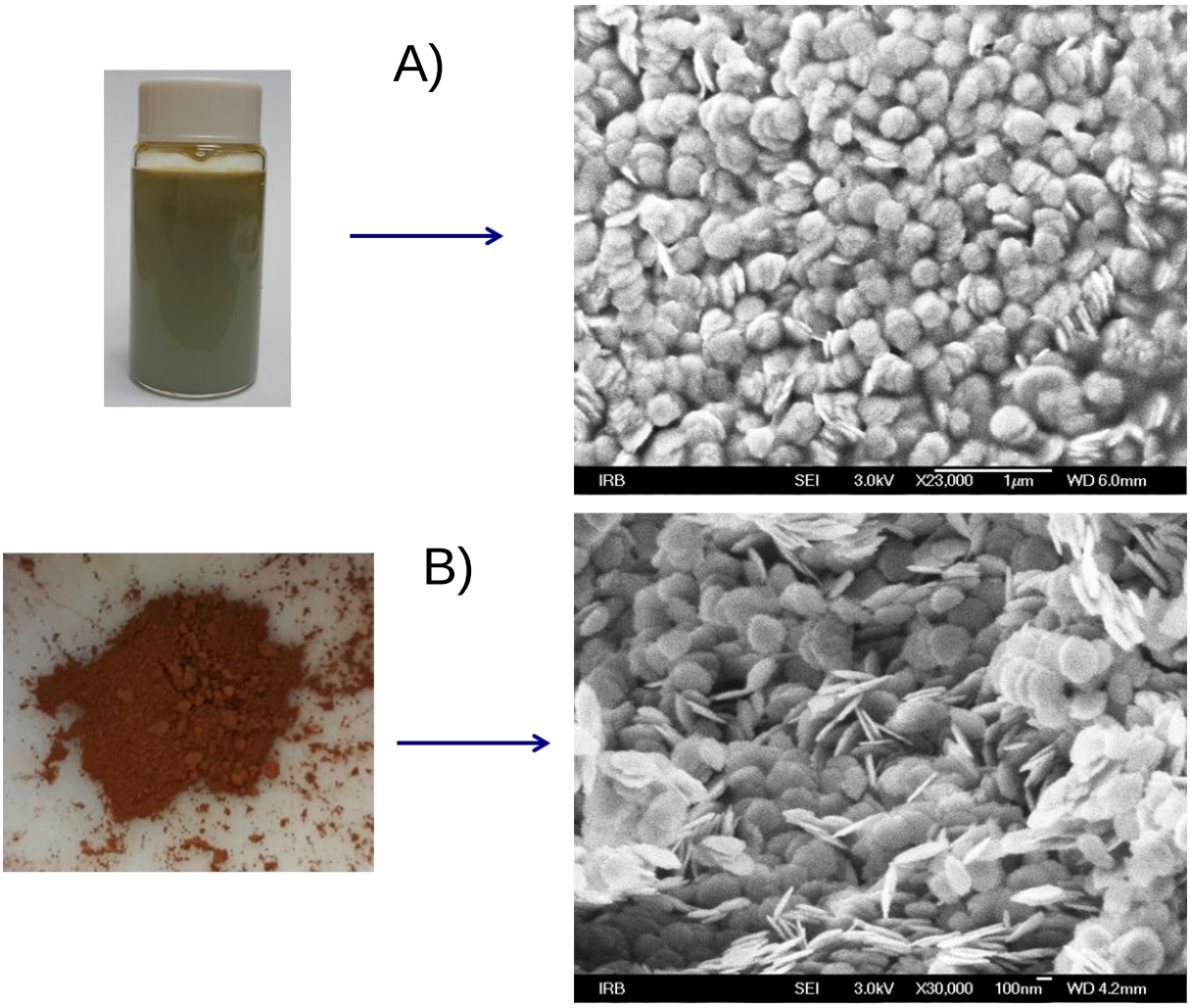

Fig. S1 SEM image of a green-gray stable suspension and corresponding photo (A). One drop of the suspension is placed on the silicon substrate, dried in air and then recorded using FE SEM (high vacuum). Since there was no isolation of solid (there were no centrifugation, washing, drying) the sample S1 contained a lot of unwashed DEAE-dextran polymer. Nanodiscs are virtually non-visible due to their embedding in larger pseudospherical particles. On the contrary, after the isolation of sample S1, the discrete disc-like nanoparticles are well visible (B).

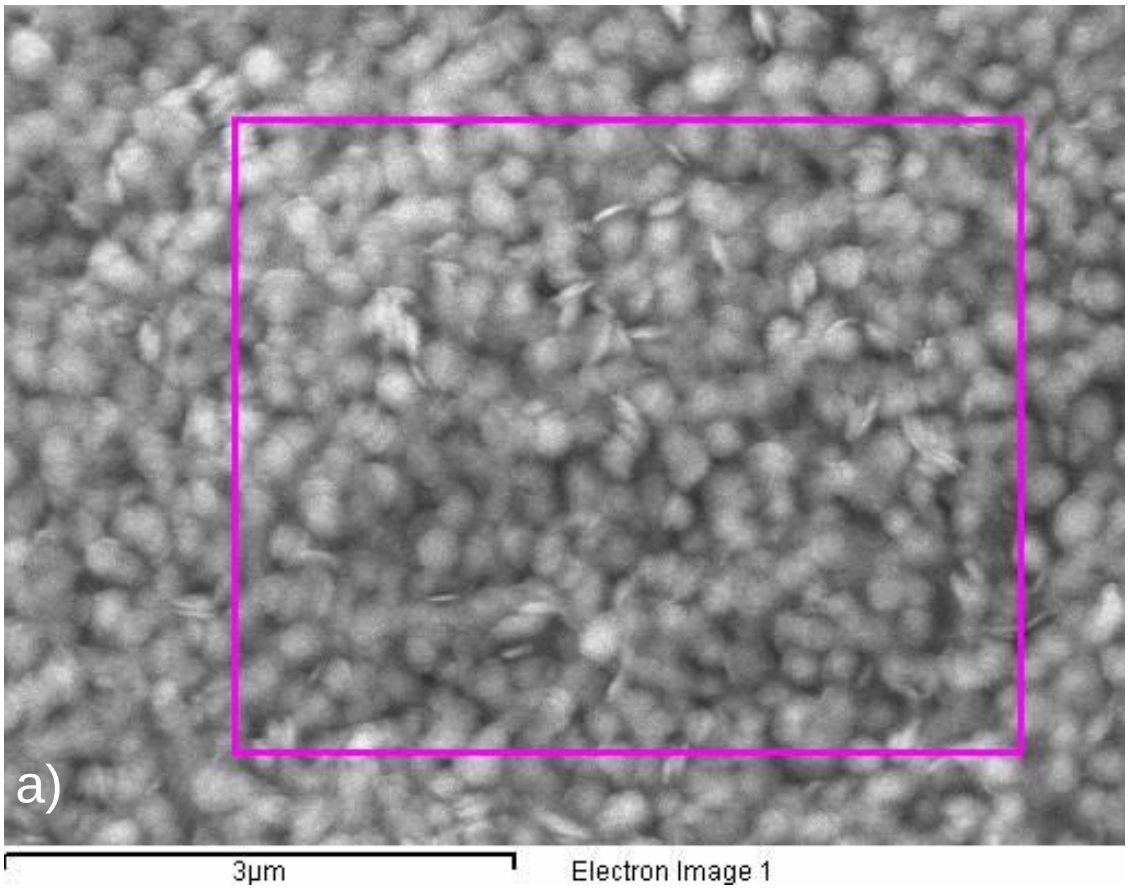

Element	Atomic%
C	40.36
O	42.86
Fe	13.11
Na	1.24
Si	0.35
Cl	2.08
Total	100.00

Fig. S2 SEM image (a) and corresponding EDS analysis of green-gray stable suspension of sample S1 (b). A drop of the suspension was placed on the carbon support and dried naturally in the air. The elemental analysis from the highlighted area is given in the table (inset). The relative concentration of carbon (C) as well as of chlorine (Cl) is high. The Fe/O relative ratio is 0.31, which is highly below the ideal Fe/O ratio of 0.5 for FeOOH. The relative high concentration of carbon (C) is very probably due to DEAE-dextran and in less extends to the carbon support. The very small amount of Si in the sample is due to the SiO_2 (leaching from chemical glasses).

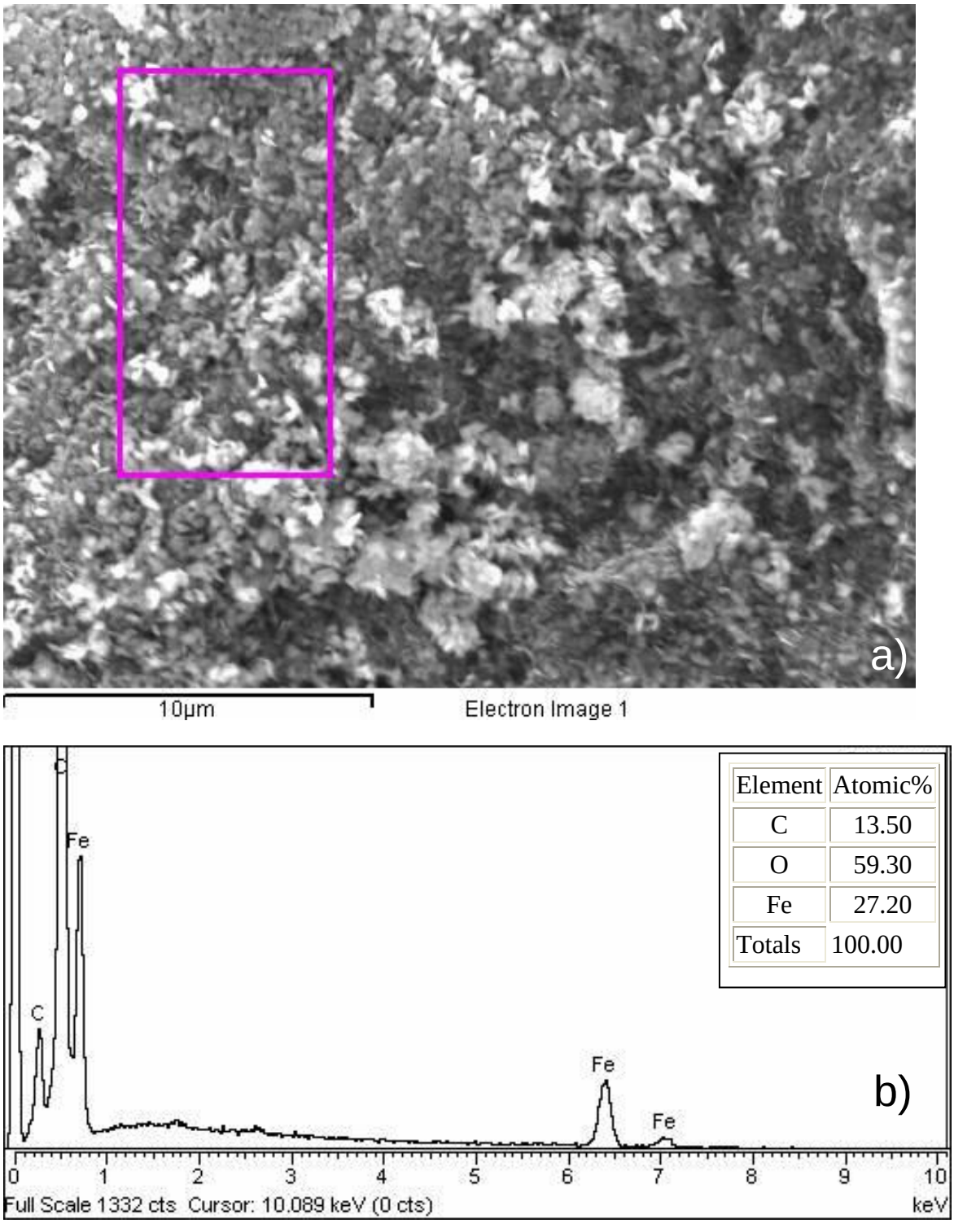

Element	Atomic%
C	13.50
O	59.30
Fe	27.20
Totals	100.00

Fig. S3 SEM image (a) and corresponding EDS analysis of sample S1 that was isolated using centrifugation, washing and drying (powder sample). The EDS analysis should be performed at voltage of 10 kV or higher and due to this reason the sample is recorded at relative low magnification (low discharge of electrons on the sample). The relative concentration of carbon (C) is low (13.50 at. %), whereas the Fe/O relative ratio is 0.45, which is slightly below the ideal Fe/O ratio of 0.5 in FeOOH. The Fe/O ratio in magnetite (Fe_3O_4) is 0.75. The relative low Fe/O ratio indicated the formation of FeOOH phase and not the formation of magnetite. The relative concentration of carbon is not accurate due to the sample being placed

on the graphite support. Nevertheless, the relative concentration of carbon is much lower than in case of EDS analysis of green-gray suspension (40.36 % of carbon in green-gray suspension, Fig. S2). In addition in the powder sample S1 there was no chlorine (Cl). Taking together the isolated powder of sample S1 consists of much less DEAE-dextran polymer and does not contain chloride ions in comparison with the green-gray stable suspension of sample S1 (Fig. S2).

Section S3 Electron Microscopy **(**HRTEM and SAED) characterization of samples S1

Sample S1

Line	r* (1/nm)	d (Å)	hkl	Intensity	Phase
1	5.800	3.4483	120	very weak	goethite
2	7.3870	2.7075	130	weak	goethite
3	7.8800	2.5381	100	strong	feroxyhyte
4	8.9430	2.2364	101	weak	feroxyhyte
5	10.9650	1.8240	230	very weak	goethite
6	11.8580	1.6866	102	weak	feroxyhyte
7	13.8270	1.4464	110	strong	feroxyhyte
8	15.7090	1.2732	200	weak	feroxyhyte

Experimental SAED (Selected Area Electron Diffraction) patterns taken from the whole area of the HRTEM (High Resolution Transmission Electron Microscope) image shown in the right-bottom corner.

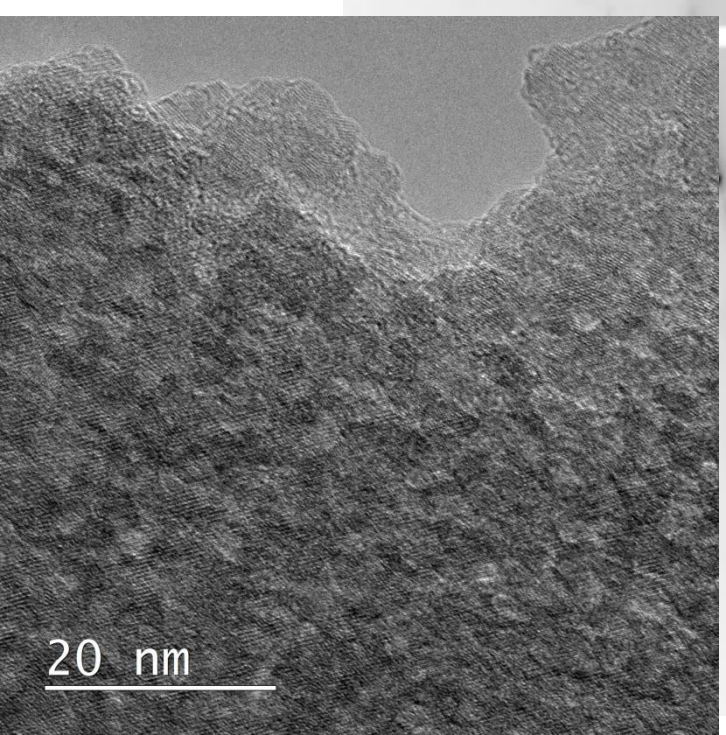

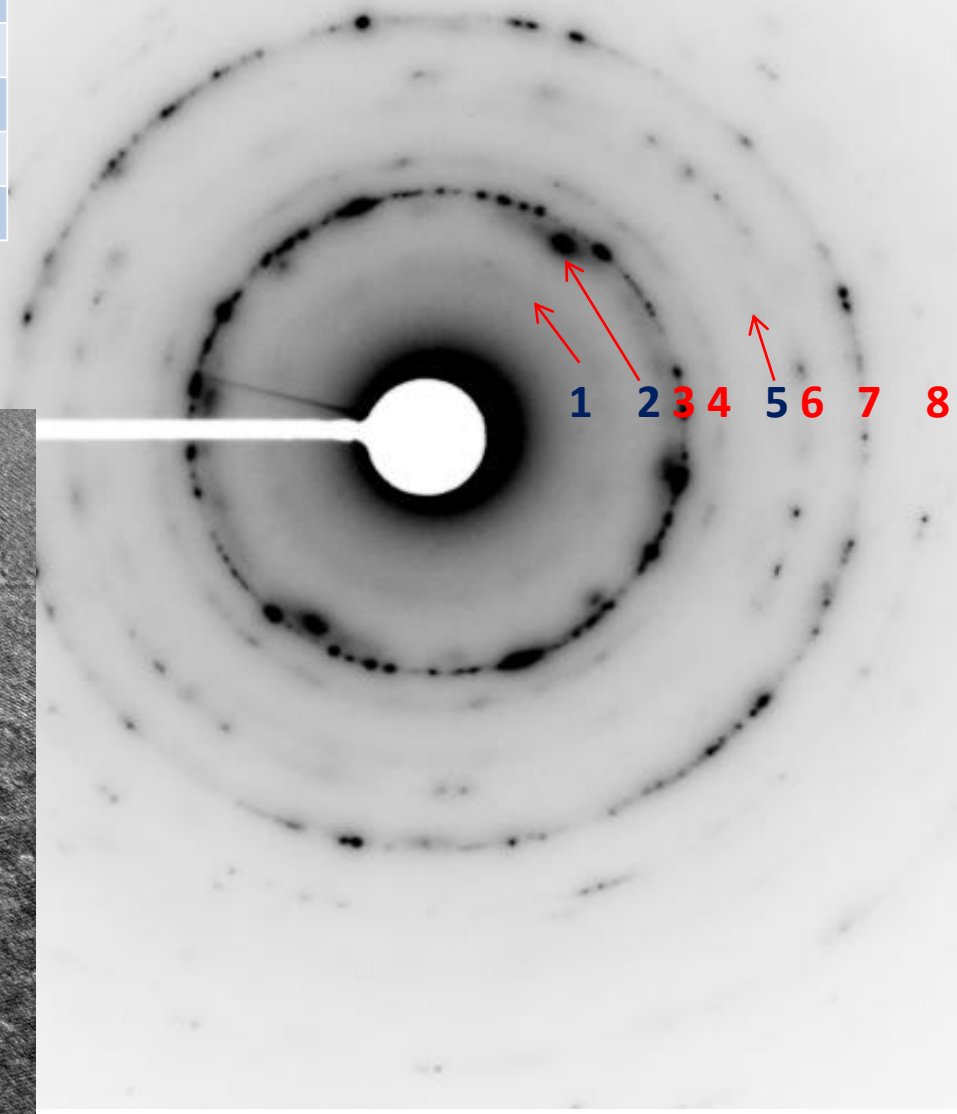

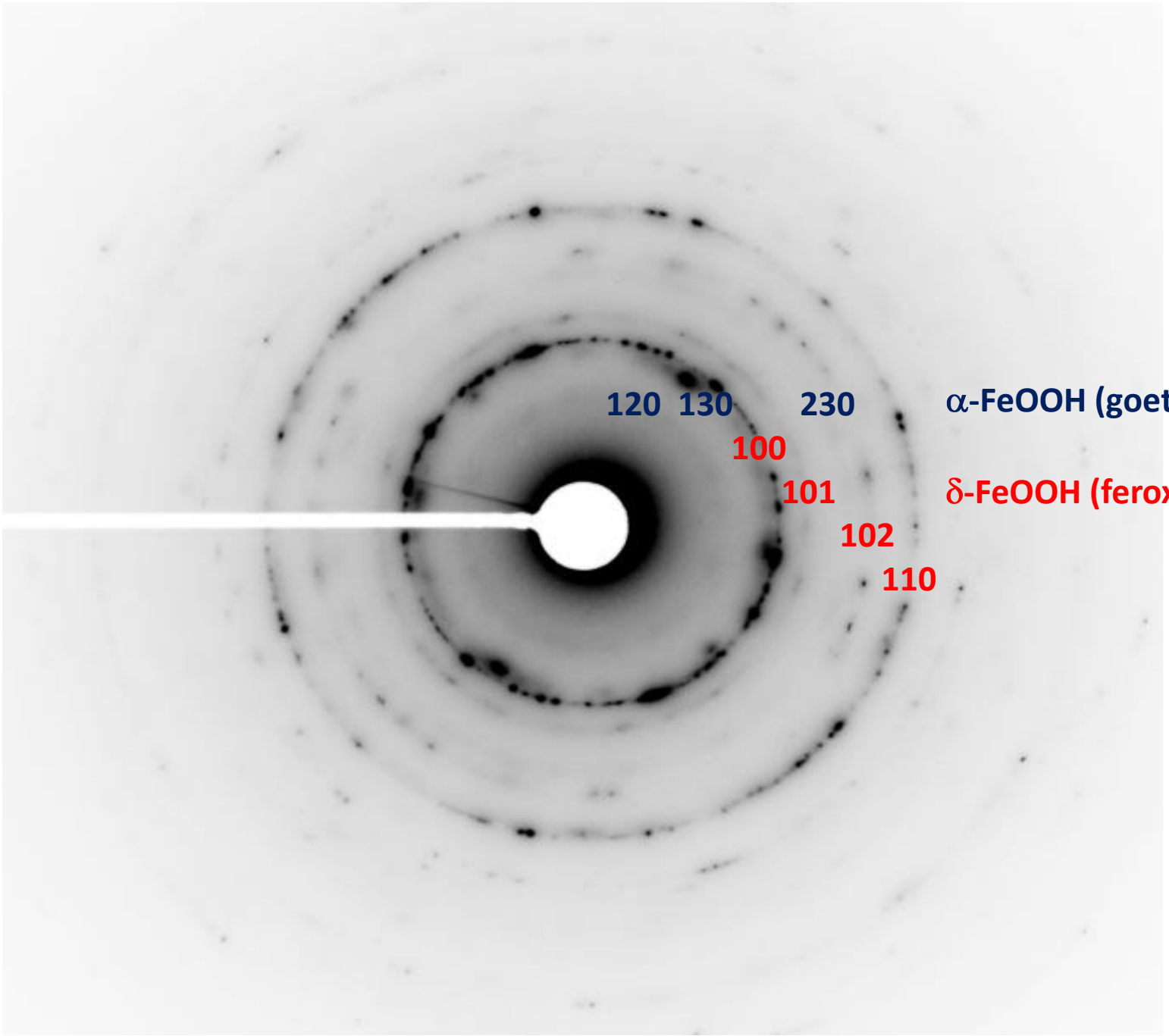
120
130
230
α-FeOOH (goethite)
100
101
δ-FeOOH (feroxyhyte)
102
110

Sample Name FeOOH_delta

Crystal system: Hexagonal Lattice Type: P

Lattice Parameter: a= 2.95 b= 2.95 c= 4.56

Lattice Parameter: Alpha= 90 Beta= 90 Gama=120

Radiation: Cu WaveLength: 1.540598

2Theta Start= 10 2Theta End= 140.0

Total 26 Lines are generated!

H	K	L	d	2Theta	SinT	SinT^2
0	0	1	4,56000	19,451	0,168925	0,028536
1	0	0	2,55477	35,097	0,301513	0,090910
0	0	2	2,28000	39,492	0,337850	0,114143
1	0	1	2,22881	40,438	0,345610	0,119446
1	0	2	1,70108	53,851	0,452828	0,205053
0	0	3	1,52000	60,899	0,506776	0,256822
1	1	0	1,47500	62,965	0,522237	0,272731
1	1	1	1,40341	66,580	0,548878	0,301267
1	0	3	1,30628	72,270	0,589688	0,347732
2	0	0	1,27739	74,174	0,603027	0,363641
1	1	2	1,23844	76,924	0,621992	0,386874
2	0	1	1,23004	77,547	0,626241	0,392177
0	0	4	1,14000	85,017	0,675701	0,456572
2	0	2	1,11441	87,453	0,691219	0,477784
1	1	3	1,05853	93,388	0,727704	0,529553
1	0	4	1,04106	95,449	0,739920	0,547482
2	0	3	0,97792	103,941	0,787695	0,620463
2	1	0	0,96561	105,828	0,797730	0,636373
2	1	1	0,94467	109,258	0,815419	0,664908
0	0	5	0,91200	115,264	0,844626	0,713393
1	1	4	0,90200	117,297	0,853992	0,729303
2	1	2	0,88916	120,068	0,866323	0,750515
1	0	5	0,85891	127,489	0,896830	0,804304
3	0	0	0,85159	129,523	0,904540	0,818193
2	0	4	0,85054	129,824	0,905656	0,820213
3	0	1	0,83712	133,905	0,920179	0,846729

Sample Name FeOOH_getit

Crystal system: Orthorombic Lattice Type: P

Lattice Parameter: a= 4.5979 b= 9.9510 c= 3.0178

Lattice Parameter: Alpha= 90 Beta= 90 Gama=90

Radiation: Cu WaveLength: 1.540598

2Theta Start= 10 2Theta End= 140.0

Total 188 Lines are generated!

H	K	L	d	2Theta	SinT	SinT^2
0	2	0	4,97550	17,813	0,154818	0,023969
1	0	0	4,59790	19,289	0,167533	0,028067
1	1	0	4,17389	21,270	0,184552	0,034059
1	2	0	3,37682	26,372	0,228114	0,052036
0	3	0	3,31700	26,857	0,232228	0,053930
0	0	1	3,01780	29,577	0,255252	0,065154
0	1	1	2,88792	30,940	0,266731	0,071146
1	3	0	2,69005	33,279	0,286351	0,081997
0	2	1	2,58028	34,739	0,298533	0,089122
1	0	1	2,52292	35,555	0,305321	0,093221
0	4	0	2,48775	36,075	0,309637	0,095875
1	1	1	2,44554	36,719	0,314981	0,099213
2	0	0	2,29895	39,153	0,335066	0,112269
1	2	1	2,25017	40,038	0,342330	0,117189
2	1	0	2,23995	40,228	0,343891	0,118261
0	3	1	2,23221	40,374	0,345084	0,119083
1	4	0	2,18801	41,226	0,352054	0,123942
2	2	0	2,08694	43,321	0,369104	0,136238
1	3	1	2,00807	45,114	0,383602	0,147150
0	5	0	1,99020	45,542	0,387046	0,149805
0	4	1	1,91959	47,317	0,401284	0,161028
2	3	0	1,88949	48,118	0,407675	0,166199
2	0	1	1,82875	49,823	0,421215	0,177422
1	5	0	1,82644	49,890	0,421749	0,177872
2	1	1	1,79863	50,716	0,428269	0,183415
1	4	1	1,77141	51,552	0,434851	0,189096
2	2	1	1,71648	53,329	0,448766	0,201391
2	4	0	1,68841	54,288	0,456228	0,208144
0	5	1	1,66143	55,244	0,463636	0,214958
0	6	0	1,65850	55,350	0,464455	0,215719
2	3	1	1,60148	57,500	0,480991	0,231352
1	5	1	1,56255	59,073	0,492976	0,243025
1	6	0	1,56011	59,174	0,493747	0,243786
3	0	0	1,53263	60,344	0,502598	0,252605
3	1	0	1,51477	61,131	0,508525	0,258597
0	0	2	1,50890	61,395	0,510504	0,260614
2	5	0	1,50469	61,585	0,511931	0,262074
0	1	2	1,49185	62,174	0,516339	0,266606
2	4	1	1,47347	63,038	0,522779	0,273297
3	2	0	1,46472	63,458	0,525903	0,276574

Sample Name Fe3O4 Magnetite

Crystal system: Cubic Lattice Type: P

Lattice Parameter: a= 8.405 b= 8.405 c= 8.405

Lattice Parameter: Alpha= 90 Beta= 90 Gama=90

Radiation: Cu WaveLength: 1.540598

2Theta Start= 10 2Theta End= 140.0

Total 152 Lines are generated!

H	K	L	d	2Theta	SinT	SinT^2
1	0	0	8,40500	10,517	0,091648	0,008399
1	1	0	5,94323	14,894	0,129609	0,016799
1	1	1	4,85263	18,267	0,158738	0,025198
2	0	0	4,20250	21,124	0,183295	0,033597
2	1	0	3,75883	23,651	0,204931	0,041997
2	1	1	3,43133	25,946	0,224490	0,050396
2	2	0	2,97162	30,047	0,259219	0,067194
2	2	1	2,80167	31,917	0,274943	0,075594
3	0	0	2,80167	31,917	0,274943	0,075594
3	1	0	2,65789	33,694	0,289816	0,083993
3	1	1	2,53420	35,391	0,303961	0,092392
2	2	2	2,42631	37,021	0,317477	0,100792
3	2	0	2,33113	38,591	0,330441	0,109191
3	2	1	2,24633	40,109	0,342914	0,117590
4	0	0	2,10125	43,011	0,366591	0,134389
3	2	2	2,03851	44,404	0,377873	0,142788
4	1	0	2,03851	44,404	0,377873	0,142788
3	3	0	1,98108	45,763	0,388828	0,151187
4	1	1	1,98108	45,763	0,388828	0,151187
3	3	1	1,92824	47,092	0,399483	0,159587
4	2	0	1,87942	48,392	0,409861	0,167986
4	2	1	1,83412	49,667	0,419983	0,176385
3	3	2	1,79195	50,918	0,429866	0,184785
4	2	2	1,71566	53,357	0,448980	0,201583
4	3	0	1,68100	54,547	0,458239	0,209983
5	0	0	1,68100	54,547	0,458239	0,209983
4	3	1	1,64836	55,720	0,467313	0,218382
5	1	0	1,64836	55,720	0,467313	0,218382
3	3	3	1,61754	56,877	0,476215	0,226781
5	1	1	1,61754	56,877	0,476215	0,226781
4	3	2	1,56077	59,147	0,493538	0,243580
5	2	0	1,56077	59,147	0,493538	0,243580
5	2	1	1,53454	60,262	0,501975	0,251979
4	4	0	1,48581	62,455	0,518438	0,268778
4	4	1	1,46312	63,535	0,526476	0,277177
5	2	2	1,46312	63,535	0,526476	0,277177
4	3	3	1,44145	64,606	0,534393	0,285576
5	3	0	1,44145	64,606	0,534393	0,285576
5	3	1	1,42070	65,666	0,542195	0,293976
4	4	2	1,40083	66,718	0,549886	0,302375

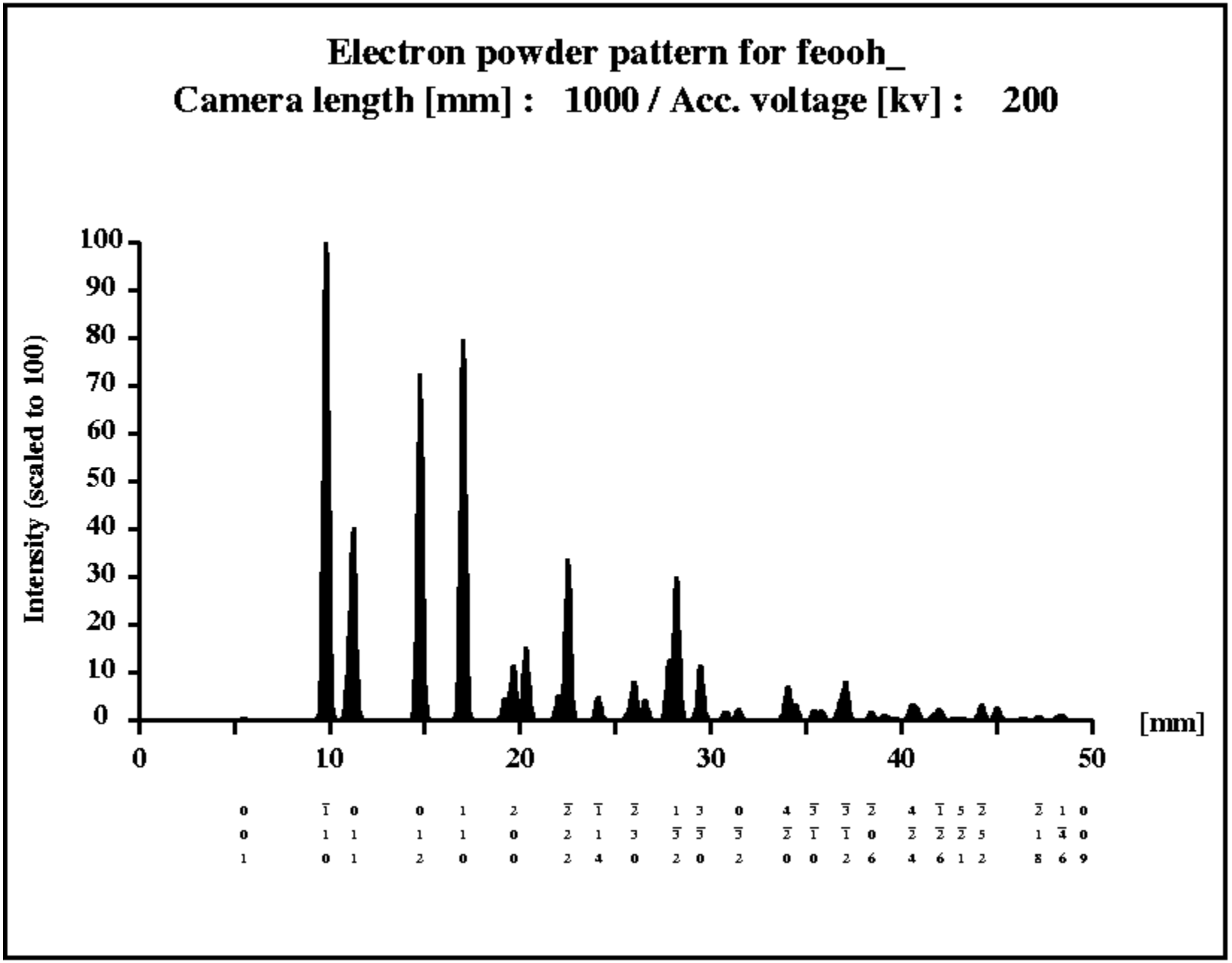

Intensity distribution - Delta-FeOOH calculations

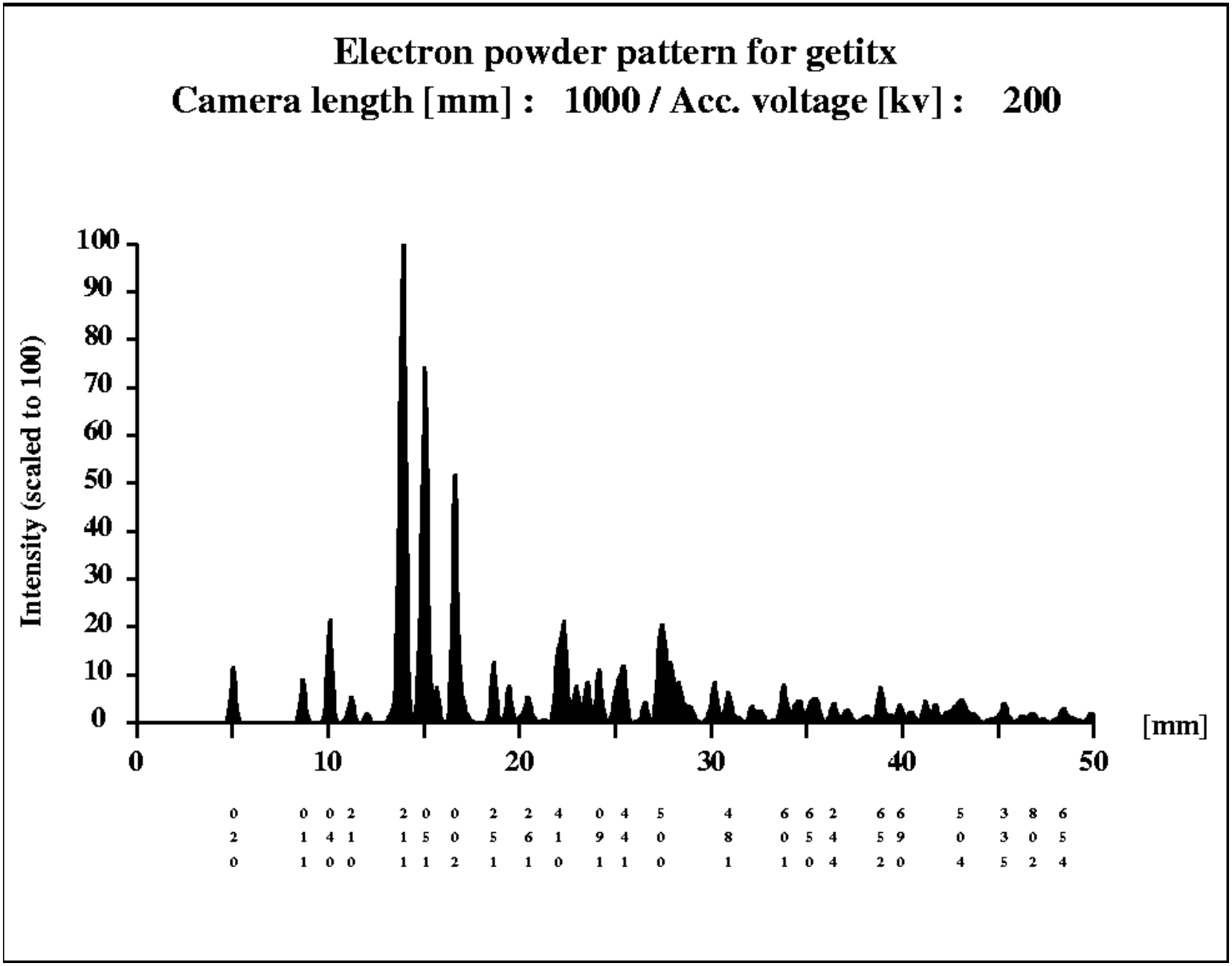

Intensity distribution - Alpha FeOOH Goethite calculations

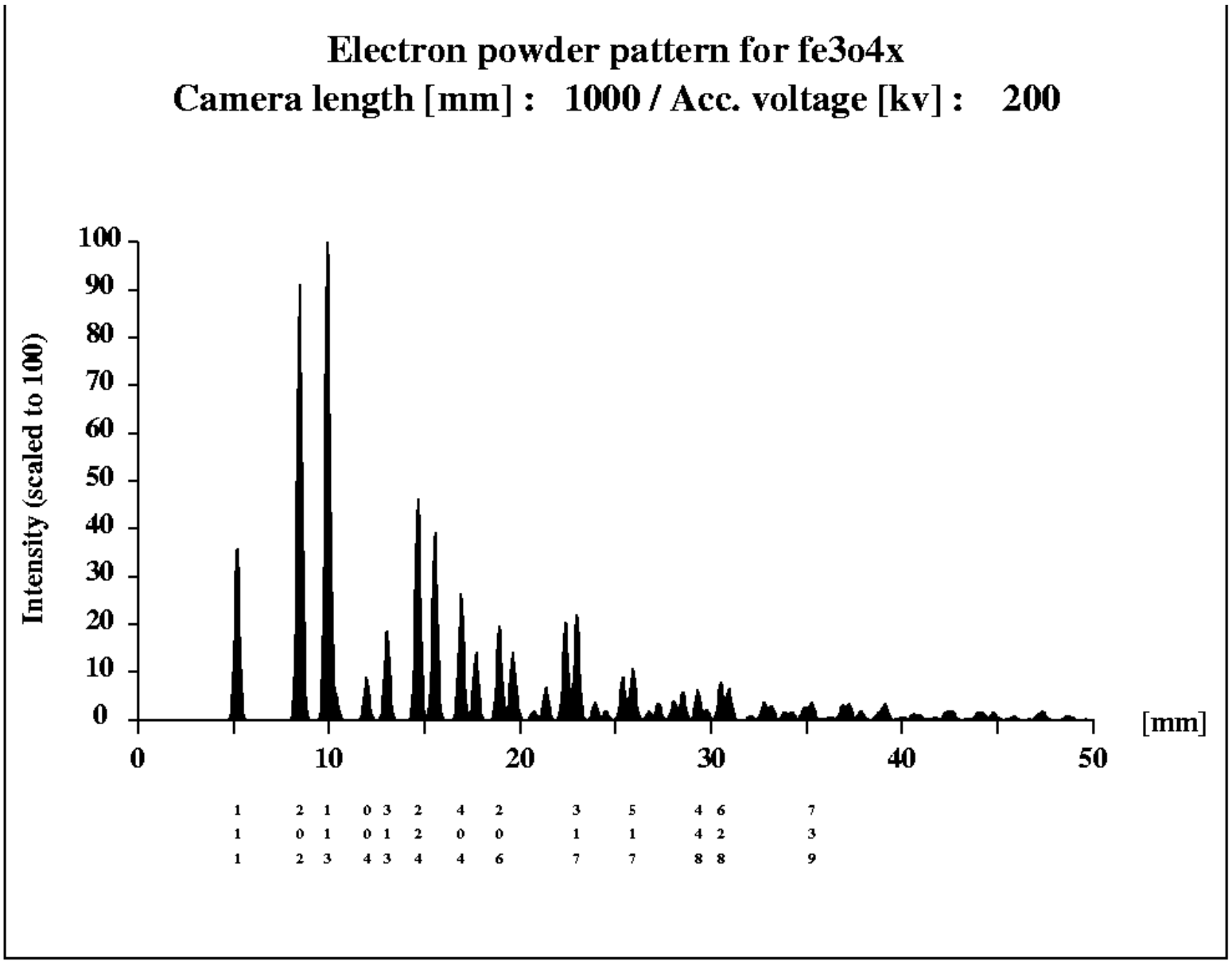

Intensity distribution - Fe_3O_4 Magnetite calculations

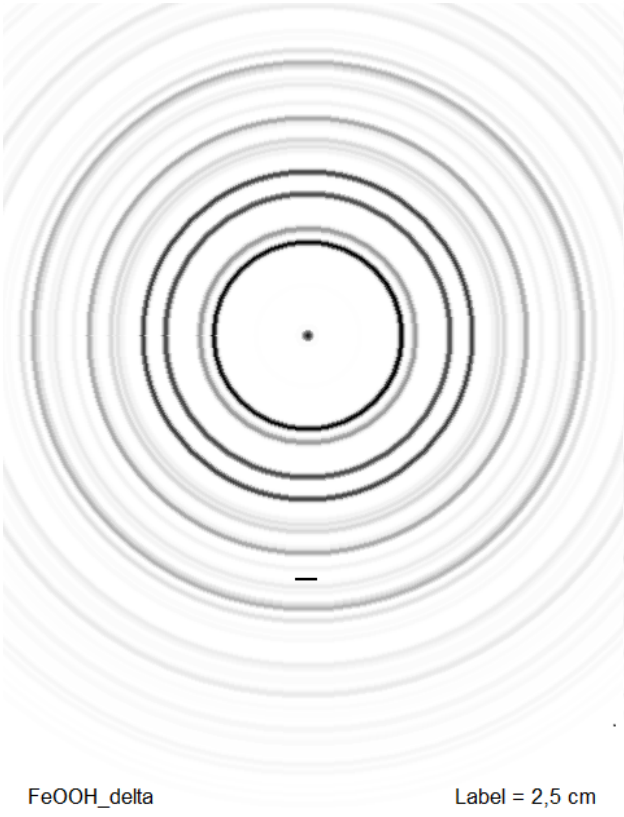

Feroxyhyte

Goethite

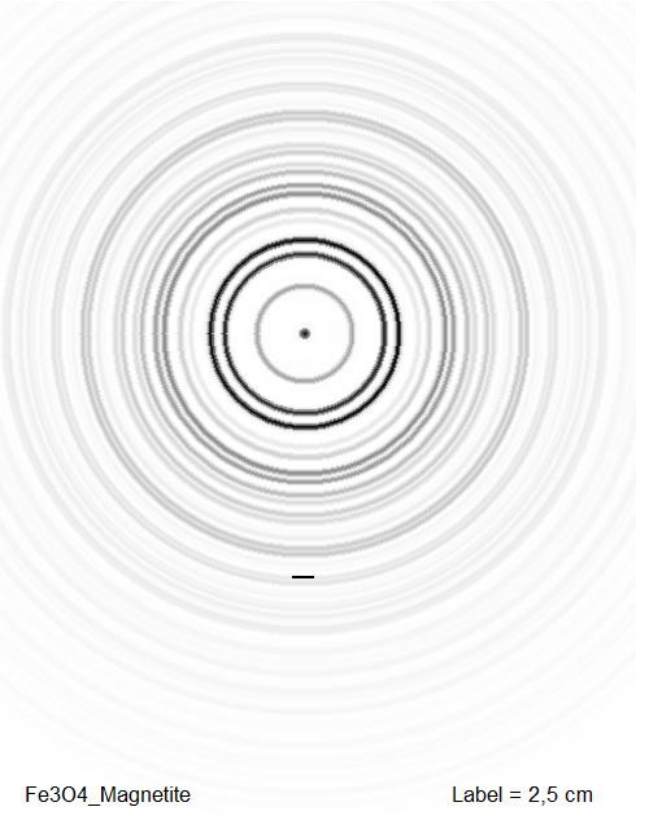

Magnetite

SAED pattern simulations

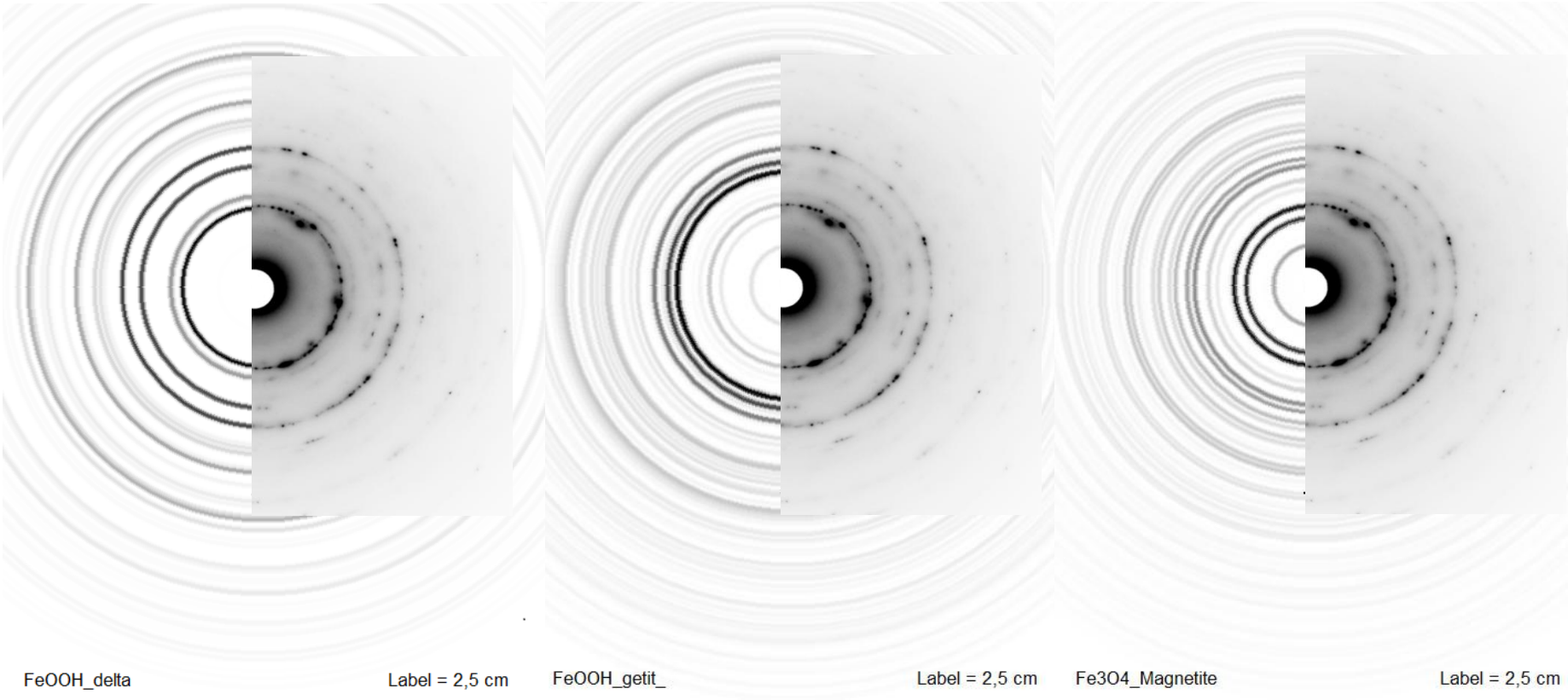

Feroxyhyte Goethite Magnetite

Comparison of SAED pattern simulations with experimentally obtained patterns of sample S1

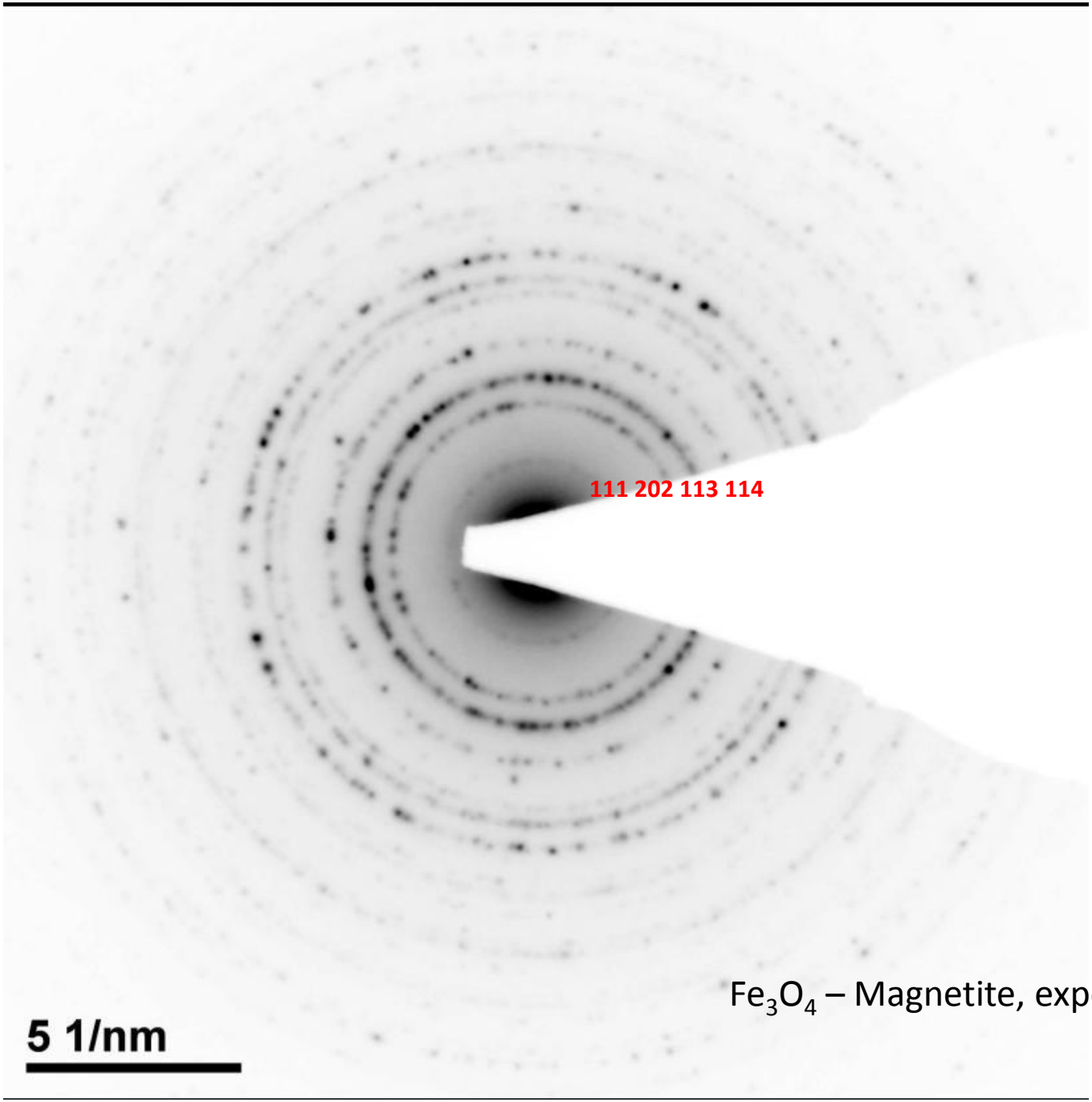

Fe_3O_4 – Magnetite, experimental

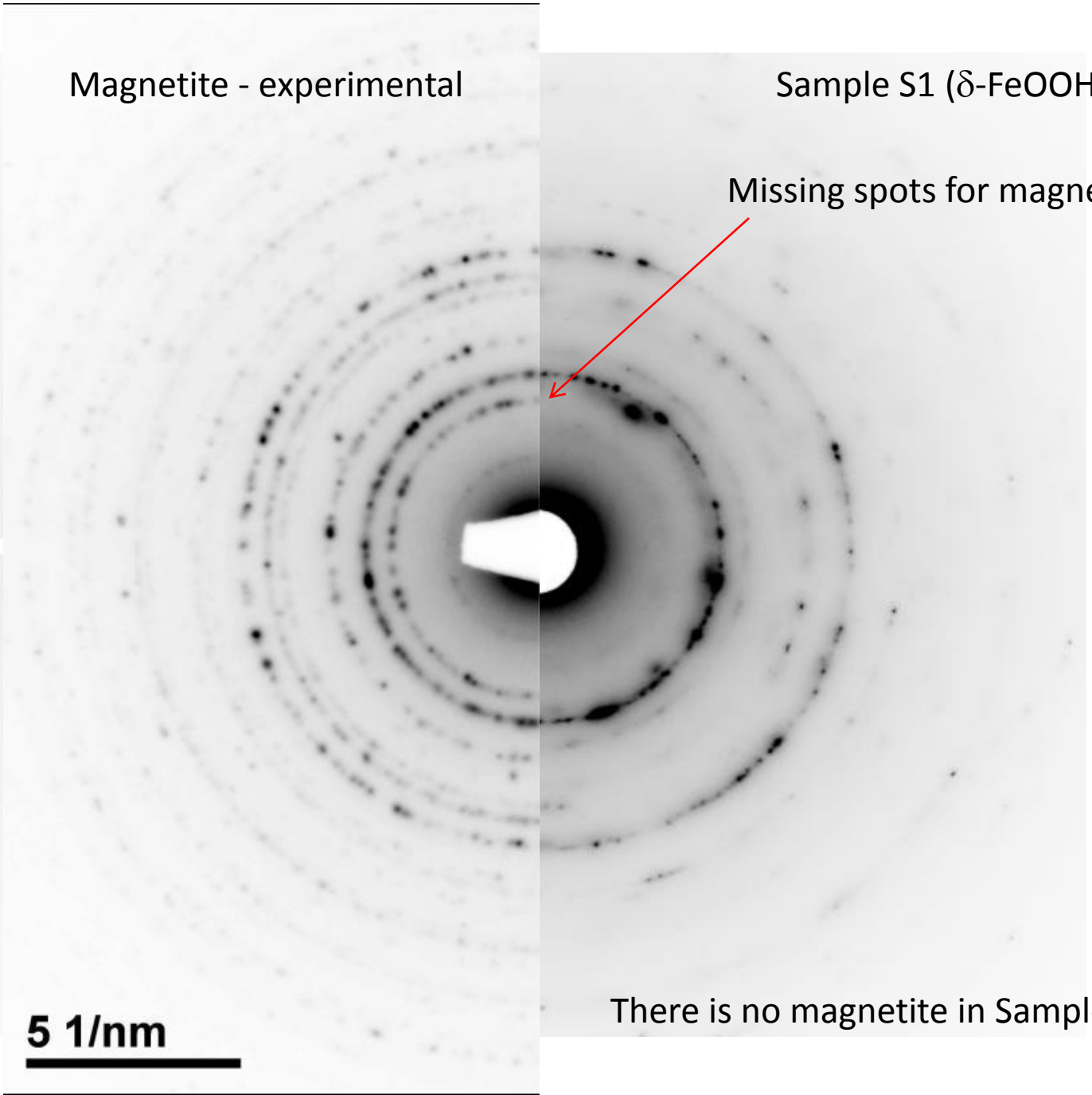

There is no magnetite in Sample 1

Section S3 *X-ray powder diffraction characterization of samples*

Quantitative crystal phase analysis

X-ray powder diffraction (XRD) patterns were recorded at 20 ^{o}C using an *ItalStructures* diffractometer APD2000 with monochromatized CuKα radiation (graphite monochromator).

Fig. S4 shows XRD powder patterns of sample S1 and S2. The XRD patterns revealed the presence of δ-FeOOH (feroxyhyte, space group $P\bar{3}m1$, a = 0.295 nm, c = 0.456 nm; *ICDD PDF card No.* 77-247) as a dominant phase and α-FeOOH (goethite, space group *Pbnm*, a = 0.426 nm, b = 0.996 nm c = 0.3022 nm; ICDD card 29-0713) as a minor phase. Rietveld refinements [1] (program MAUD [2]) of powder diffraction patterns were used for a quantitative crystal phase analysis (Fig. S4). Crystallographic information files (CIF) for α-FeOOH and δ-FeOOH, used in the Rietveld refinements, were taken from papers [3] and [4]. Graphical representations of the final Rietveld refinements of samples S1 and S2 are shown in Fig. S4. In both cases the R_{wp} indices with subtracted background were below 8% which indicate good quality of least squares refinement. Volume fraction of δ-FeOOH in the samples S1 and S2 were estimated at 0.71(2) and 0.73(2), respectively.

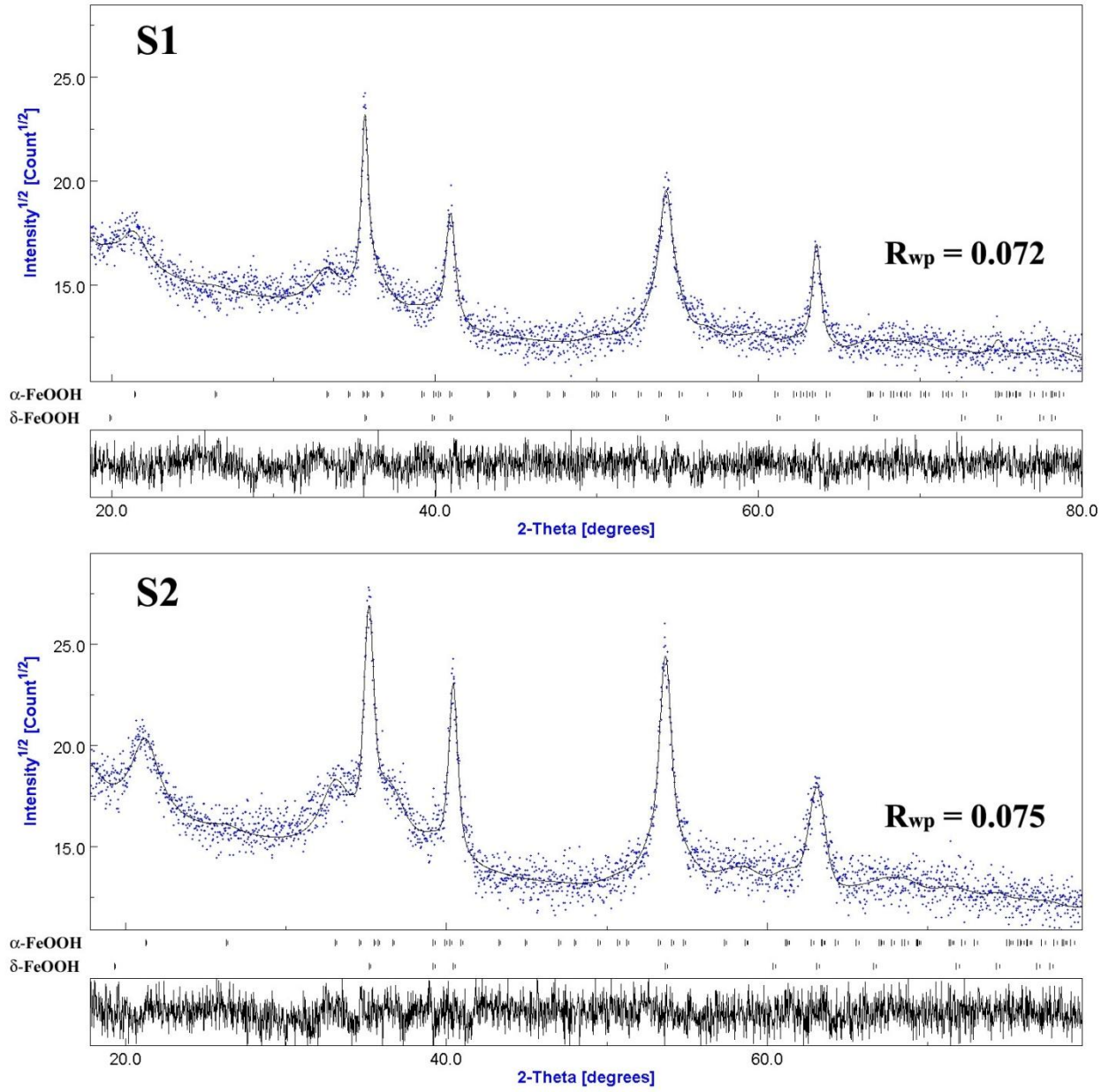

Fig. S4 XRD powder patterns of sample S1 and S2. The XRD patterns revealed the presence of δ-FeOOH (feroxyhyte) with volume fraction of 0.71(2) and 0.73(2), in sample S1 and S2, respectively and α-FeOOH (goethite) with volume fraction of 0.29(2) and 0.27(2), in sample S1 and S2, respectively

Precise lattice parameters determination of δ-FeOOH

Precise lattice parameters of δ-FeOOH phase in the samples S1 and S2 were determined from the results of Le Bail refinements [5] (program GSAS [6] with a graphical user interface EXPGUI [7]) of powder diffraction patterns. Silicon (*Koch-Light Lab. Ltd.*) was used as an internal standard (space group $Fd\bar{3}m$; a = 5.43088 Å; *ICDD PDF card No. 27-1402*). XRD pattern of the sample and ~5% of silicon was collected over a 2θ range from 15 to 80° with a step of 0.025°. A graphical representation of the final Le Bail refinements is shown in **Fig. S5**. The R_{wp} indices with subtracted background of the refined patterns were 0.055 and 0.053 for samples S1 and S2, respectively, which indicate very good quality of least squares refinement. List of the 2θ positions and d_{hkl} values of four most prominent *hkl* reflections of δ-FeOOH phase in samples S1 and S2 and the corresponding values from *ICDD PDF card No.* 77-0247 are given in Table S1 in Suppl. data. The obtained values of lattice parameters (a = 0.2943(2) nm; c = 0.4572(1) nm; V = 0.03429(1) nm^3 for δ-FeOOH phase in sample S1 and a = 0.2949(1) nm; c = 0.4603(1) nm; V = 0.03467(1) nm^3 for δ-FeOOH phase in sample S2) indicate small increase of the δ-FeOOH unit-cell parameters in the sample S2.

Table S1: The *hkl* indices, the 2θ positions and the d_{hkl} values of four most prominent diffraction lines of δ-FeOOH in samples S1 and S2 and the corresponding values from *ICDD PDF card No.* 77-0247.

δ-FeOOH	**Card No. 77-0247**		**Sample S1**		**Sample S2**	
hkl	**2θ/°**	**d_{hkl}/ nm**	**2θ/ °**	**d_{hkl}/ nm**	**2θ/°**	**d_{hkl}/ nm**
100	35.125	0.25548	35.24	0.2547	35.13	0.2554
101	40.471	0.22288	40.54	0.2225	40.39	0.2233
102	53.895	0.17011	53.89	0.1701	53.60	0.1710
110	63.020	0.14750	63.21	0.1471	63.04	0.1475

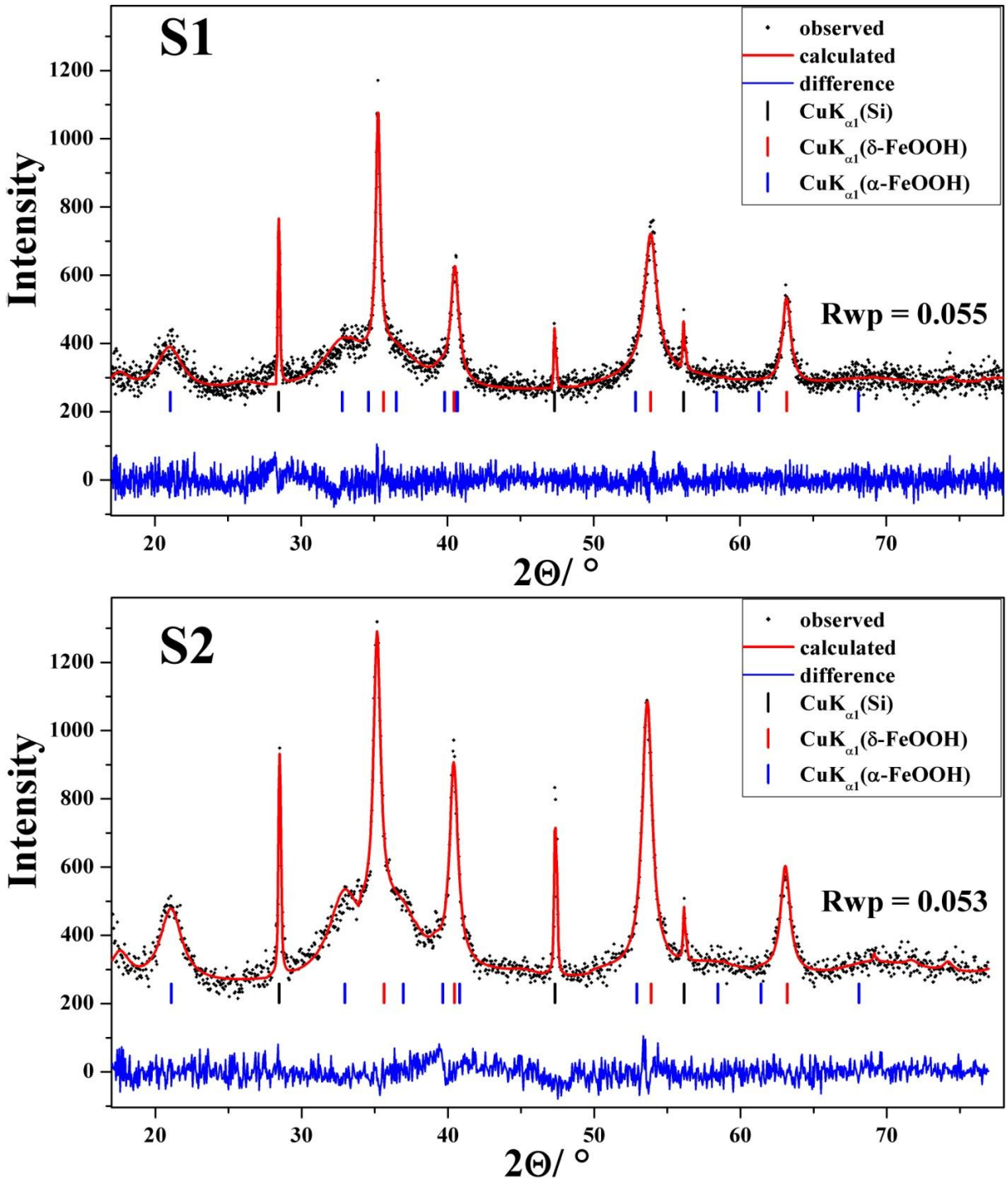

Fig. S5 XRD patterns of the sample S1 and S2 with the ~5% of silicon using as internal standard. The R_{wp} indices with subtracted background of the refined patterns were 0.055 and 0.053 for samples S1 and S2, respectively, which indicate very good quality of least squares refinement. List of the 2θ positions and d_{hkl} values of four most prominent *hkl* reflections of δ-FeOOH phase in samples S1 and S2 and the corresponding values from *ICDD PDF card No.* 77-0247 are given in Table 1

Line broadening analysis

The results of line broadening analysis indicate the presence of size anisotropy in the δ-FeOOH crystallites of sample S1. Significantly smaller full width at half maximum (FWHM) value of the δ-FeOOH line 100 compared to the relatively close diffraction line 101 (**Table S2**) indicate that crystals are more elongated along the *a*-axis compared to the *c*-axis. The crystallite sizes were estimated from the Scherrer equation:

$$D_{hkl} = \frac{0.9\lambda}{\beta_{hkl} \times \cos\theta}\ , \qquad (1)$$

where D_{hkl} is a volume average of the crystal thickness in the direction normal to the reflecting plane *hkl*, λ is the X-ray wavelength (CuKα), θ is the Bragg angle and β_{hkl} is pure full width of the diffraction line (*hkl*) at half the maximum intensity. In case of the sample S1 the D_{100} value was estimated at ~31 nm and the D_{101} value at ~12 nm. This result is in accordance with anisotropic disc-like morphology of sample S1 (Fig. 1a and Fig. S1B). On the contrary, the calculated average crystallite sizes of the 100 and 101 lines of δ-FeOOH in sample S2 are very similar (D_{100} ~16 nm and D_{101} ~15 nm), which indicates the dominance of the 3D morphology in this sample.

Diffraction lines of α-FeOOH (goethite) in both samples S1 and S2 appeared to be very broad, which indicate presence of ultrasmall nanoparticles of goethite. The crystallite sizes were estimated from broadening of the most prominent diffraction line of goethite (line 110) at ~4.2 nm and ~5.1 nm in samples S1 and S2, respectively.

Table S2: The *hkl* indices, the 2θ positions, the FWHM values and the D_{hkl} values (estimated from Scherrer equation) of the four most prominent diffraction lines of δ-FeOOH in samples S1 and S2.

Sample S1 (δ-FeOOH)			
hkl	**2θ / °**	**FWHM/ °**	**D_{hkl}/ nm**
100	35.24	0.26	~31
101	40.54	0.67	~12
102	53.89	1.11	~8
110	63.21	0.55	~17
Sample S2 (δ-FeOOH)			
hkl	**2θ / °**	**FWHM/ °**	**D_{hkl}/ nm**
100	35.13	0.53	~16
101	40.39	0.56	~15
102	53.60	0.74	~12
110	63.04	0.89	~11

References

[1] H. M. Rietveld, J. Appl. Cryst., 1969, 2, 65–71.

[2] L. Lutterotti, S. Matthies and H.-R. Wenk, MAUD (Material Analysis Using Diffraction): A User Friendly Java Program for Rietveld Texture Analysis and More, in: Proceeding of the Twelfth International Conference on Textures of Materials (ICOTOM-12), vol. 1, 1999, p. 1599.

[3] W. Hoppe, Zeitschrift fur Kristallographie 103 (1940) 73-89.

[4] G. Patrat, F. de Bergevin, M. Pernet, J. Joubert, Acta Crystallographica B39 (1983) 165-170.

[5] A. Le Bail, H. Duroy and J.L. Fourquet, Mater. Res. Bull., 1988, 23, 447–452.

[6] A. C. Larson and R. B. Von Dreele, General Structure Analysis System GSAS, Los Alamos National Laboratory Report, 2001.

[7] B. H. Toby, J. Appl. Cryst., 2001, 34, 210–213.